How Does Spin Rate Affect The Trajectory of A Ping Pong Ball in Air?

Zhengxi Li

1 Introduction

The Magnus effect, which describes the lateral deflection of spinning objects due to aerodynamic forces, has been extensively studied across various fields such as sports and engineering. Early research by Briggs [1] focused on baseballs, demonstrating that deflection is directly proportional to both spin rate and the square of wind speed. His work highlighted the contrast between smooth and rough baseballs: roughened balls exhibited the expected Magnus effect, while smooth balls displayed an opposite deflection at lower speeds, underscoring the influence of surface characteristics.

Studies on soccer balls further delved into the complexities introduced by spin and surface features. Barber et al. [2] conducted a numerical study of soccer ball aerodynamics, investigating unpredictable lateral movements, such as the "banana kick," which are influenced by factors such as seam size, panel shape, and symmetry. These factors affect the drag, lift, and side forces acting on the ball.

Timkova and Jeskova [3] advocated for simpler experimental setups to demonstrate the Magnus effect in classrooms, emphasizing its educational value. Their work helped bridge the gap between theoretical physics and practical applications, making the concept more accessible and engaging.

Spathopoulos [4] applied Computational Fluid Dynamics (CFD) to simulate soccer ball trajectories, using CAD models validated by wind tunnel tests. The study illustrated the impact of ball orientation and surface geometry on aerodynamic forces, providing insights into how features like panel number affect ball flight.

Kray et al. [5] investigated the Magnus effect on soccer balls at high Reynolds numbers, revealing that force coefficients vary significantly with spin rates and boundary layer conditions. Their findings highlighted the dependence of Magnus forces on whether the boundary layer is laminar or turbulent, contributing to a better understanding of how spin impacts aerodynamic forces.

As an enthusiast of sports, particularly ball games, I find the Magnus effect intriguing. In ping pong (table tennis ball), players impart spin on the ball to make the trajectory harder for opponents to predict. The spin influences not only the interaction with the surface of the table but also the aerodynamic forces acting on the ball during flight.

2 Research Question

This paper aims to investigate that how does the spin rate affect the trajectory of a ping pong ball in air.

3 Hypothesis

As the spin rate increases, the trajectory of the ball will deviate more from the simulated trajectory.

3.1 Hypothetic Modes

3.1.1 Initial Translational Velocity and Angular Velocity

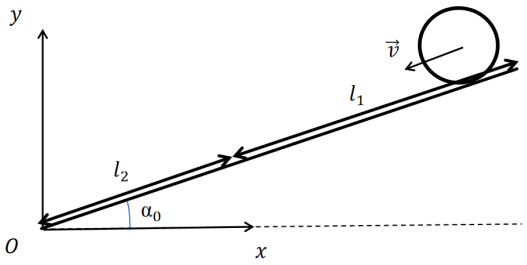

Figure 1: The slope covered by abrasive papers and oil

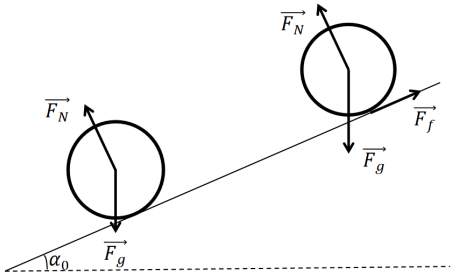

Figure 2: Forces acting on the rolling ball and the slipping ball

The ping pong ball is released from the top of the slope. The angle between x axis and the slope is α_0. The slope is covered by abrasive papers over a length l_1, followed by oil over a length l_2. Abrasive papers provide enough frictional force to make the ball roll without slipping. Oil reduces friction between the surface and the ball by minimizing their contact. As Figure 2 shown, on the slope, the frictional force $\vec{F_f}$ is applied on the contact point between the ball and the slope. Additionally, the gravitational force $\vec{F_g}$ and the normal force $\vec{F_N}$ act on the ball.

The velocity v_r—rolling a distance l_1 without slipping—is determined using energy conservation.

$$\begin{aligned} E_P &= K_{rot} + K_{trans} \\ mgl_1 \sin\alpha_0 &= \frac{1}{2}I\omega^2 + \frac{1}{2}m{v_r}^2 \end{aligned} \tag{1}$$

Since the ping pong ball is hollow, its moment of inertia is given by $\frac{2}{3}mr^2$. As the ball rolls without slipping, the angular velocity ω is equal to the translational velocity v_r divided by the radius r. Thus, the equations above is rearranged to:

$$\begin{aligned} mgl_1 \sin\alpha_0 &= \frac{1}{2}(\frac{2}{3}mr^2(\frac{v_r}{r})^2) + \frac{1}{2}m{v_r}^2 \\ mgl_1 \sin\alpha_0 &= \frac{1}{3}m{v_r}^2 + \frac{1}{2}m{v_r}^2 \\ v_r &= \sqrt{\frac{6gl_1 \sin\alpha_0}{5}} \end{aligned} \tag{2}$$

With the translational velocity, the angular velocity is represented as:

$$\omega = \frac{1}{r}\sqrt{\frac{6g \sin\alpha_0 l_1}{5}} \tag{3}$$

The initial translational velocity v_0 when it leaves the slope is v_r plus the velocity gained after traveling a distance l_2:

$$
\begin{aligned}
v_0 &= v_r + \sqrt{\frac{2E_{P2}}{m}} \\
v_0 &= \sqrt{\frac{6gl_1 \sin\alpha_0}{5}} + \sqrt{\frac{2mgl_2 \sin\alpha_0}{m}} \\
v_0 &= \sqrt{2g \sin\alpha_0} \cdot (\sqrt{\frac{3}{5}l_1} + \sqrt{l_2})
\end{aligned} \tag{4}
$$

Importantly, l_1 and l_2 together determine the initial translational velocity v_0, and l_1 solely determines the angular velocity ω. Hence, angular velocity ω can be changed by adjusting the value of l_1, and the translational velocity v_0 can be kept unchanged by adjusting the value of l_2 following this relationship by remaining $\sqrt{\frac{3}{5}l_1} + \sqrt{l_2}$ constant.

3.1.2 Force Analysis

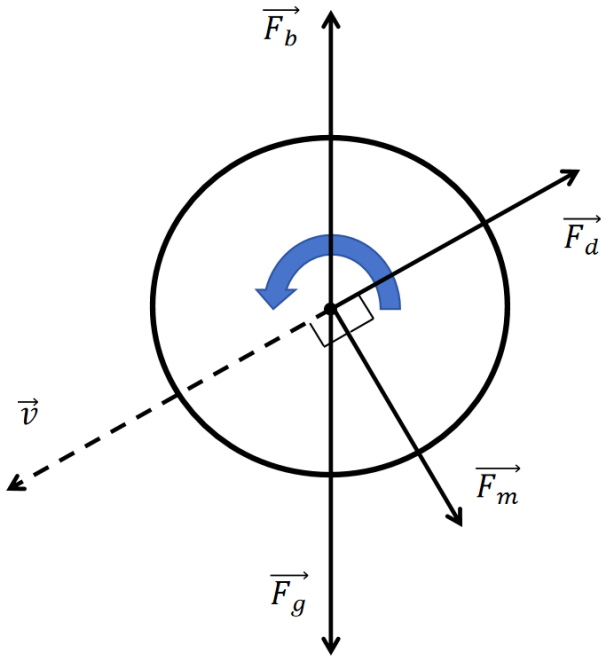

Figure 3: Free Body Diagram

According to Briggs, "any spinning ball traveling through the air experiences at least four forces: the gravitational force $\vec{F_g}$, the aerodynamic drag force $\vec{F_d}$, the buoyant force $\vec{F_b}$, and the Magnus force $\vec{F_m}$" [1].

The gravitational force is defined as:

$$\vec{F_g} = mg \tag{5}$$

For light objects, like the ping pong ball, the drag force depends on the velocity following the quadratic relationship, and the direction is opposite to the velocity [3].

$$\vec{F_d} = -k_d v^2 \tag{6}$$

The constant k_d depends on the object and the surrounding fluid properties [3]. It is expressed as $k_d = \frac{1}{2}C_d A\rho$, in which A is the cross-sectional area of the ball, ρ is the density of the air, and C_d is

a constant determined by the Reynolds number [3]. This paper defines C_d as 0.7, which is same with the one used by Timkova's experiments [3].

The buoyant force F_b is equal to the weight of the air displaced by the ball.

$$\begin{aligned} \vec{F_b} &= \rho g V_{ball} \\ &= \frac{4}{3}\pi\rho g r^3 \end{aligned} \tag{7}$$

The Magnus force $\vec{F_m}$ is a force applied by the air due to the rotation motion. More specifically, a rotating ball imparts a spinning motion to a thin layer of air surrounding to the surface of the ball. This thin layer affects the manner of flowing air which is separated by the curve of the ball. The air flow moves faster and thus farther around the curve on the side moving with this air flow layer than on the side traveling against this air flow layer [3]. Therefore, the air is deflected by the ball to the side moving with this air flow layer, and the air applies an opposite force to the ball [3].

$$\vec{F_m} = k_m v^2 \tag{8}$$

The constant k_m is defined as $k_m = \frac{1}{2}C_m A\rho$, in which A is the cross-sectional area of the ball, ρ is the density of the air, and $C_m = \frac{k_u \omega r}{v}$ [3]. According to Timkova [3], "the constant k_u is the proportionality constant between C_m and spin parameter $s = \frac{\omega r}{v}$." This paper defines k_u as 0.75, which is same with the one defined by Timkova's experiments [3].

In addition, the angular velocity ω can be assumed to be constant during the falling, even though the contact between the air causes frictional force, which may influence its value [3].

Therefore, by using Newton's second law $\vec{F} = ma$ and force equations above, the state of motion at any time can be derived:

$$\begin{cases} v_x := v_x + \int a_x dt \\ v_y := v_y + \int a_y dt \end{cases} \tag{9}$$

These differential equations will can solved and the ideal trajectory can be shown by iteration, in order to do the simulation.

3.2 Simulation

The simulation for this paper was conducted using MATLAB. The lack of an analytical solution for the ideal trajectory necessitated a numerical approach. The simulation utilized a time-stepping method with a time increment of 0.001 s to ensure accuracy. During each iteration, the forces acting on the ball and its resulting motion were calculated to determine its position. Assumed values for certain air properties were used in the simulation (see the table below).

While these assumptions introduce deviations between the simulation and experimental results, they were not experimentally validated in this paper but will be discussed in the "Errors and Limitations" section.

Additionally, the iterative simulation method has inherent limitations, particularly in its inability to fully replicate real-world conditions, which might lead to uncertainty in subsequent comparisons and affect trajectory analysis: note that due to the lack of an analytical solution, the simulation results were selected with the closest y values with the experimental results in comparison, which introduces uncertainty.

Constant	Value	Description
dt	$0.001\,\mathrm{s}$	Time step
r	$0.02\,\mathrm{m}$	Ball radius
α_0	$\arcsin(0.308)$	Angle of incline
m	$\mathrm{kg}\ 2.7 \times 10^{-3}\,\mathrm{kg}$	Mass of ball
ρ	$1.2\,\mathrm{kg\,m^{-3}}$	Air density
l_{tot}	$1.2\,\mathrm{m}$	Total length of incline
g	$9.8\,\mathrm{m\,s^{-2}}$	Gravitational acceleration
A	πr^2	Cross-sectional area
C_d	0.7	Drag coefficient
k_u	0.75	Proportionality constant
V	$\frac{4}{3}\pi r^3$	Volume of ball

Table 1: Constants Used in the Equations

Equation	Description
$l_1 + l_2 \leq l_{tot}$	Slope length limit
$v_0 = \sqrt{2g\sin\alpha_0} \cdot (\sqrt{\frac{3}{5}l_1} + \sqrt{l_2})$	Initial translational velocity
$\omega = \frac{1}{r}\sqrt{\frac{6g\sin\alpha_0 l_1}{5}}$	Angular velocity
$F = F_g + F_b + F_d + F_m = ma$	Total force equation
$F_d = k_d v^2$	Drag force
$C_m = k_u \frac{\omega r}{v}$	Calculation of Magnus coefficient
$F_m = k_m v^2$	Magnus force
$F_b = \frac{4}{3}\pi r^3 \rho g$	Buoyant force
$F_x = -k_d v^2 \cos\alpha - k_m v^2 \sin\alpha$	Force in the x direction
$F_y = -mg + \frac{4}{3}\pi r^3 \rho g + k_d v^2 \sin\alpha - k_m v^2 \cos\alpha$	Force in the y direction
$a_x = \frac{F_x}{m}$	Acceleration in the x direction
$a_y = \frac{F_y}{m}$	Acceleration in the y direction
$v_x = v_x + a_x dt$	Update of velocity in the x direction
$v_y = v_y + a_y dt$	Update of velocity in the y direction
$v = \sqrt{v_x^2 + v_y^2}$	Magnitude of velocity
$\alpha = \arccos\left(\frac{v_x}{v}\right)$	Calculation of angle of velocity relative to x axis
$x := x + v_x dt$	Update of position in the x direction
$y := y + v_y dt$	Update of position in the y direction

Table 2: Non-Constant Equations Used in The Model

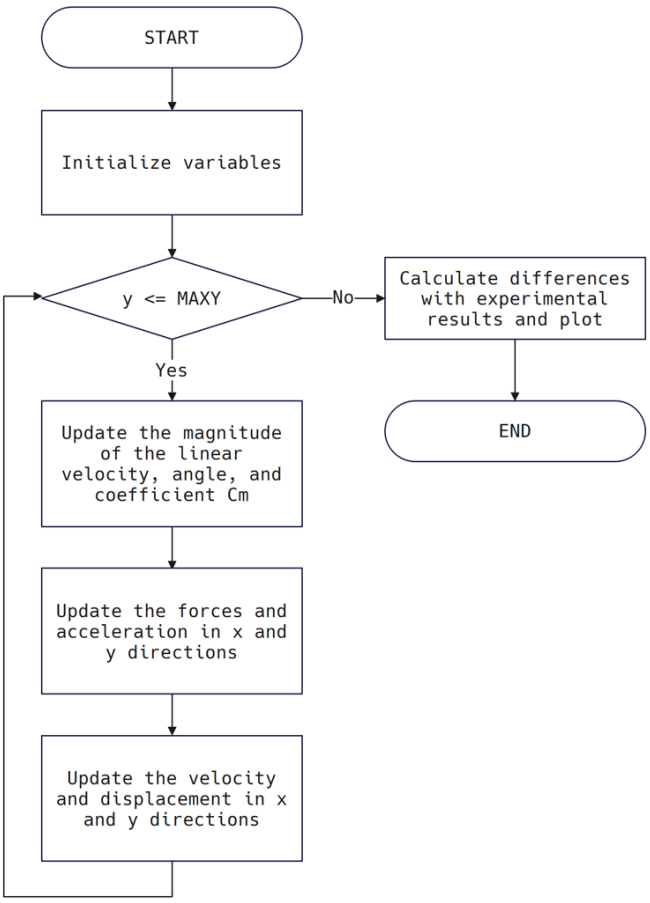

Figure 4: The Flowchart of Simulation

4 Variables

1. **Independent Variable**: The independent variable in this investigation is the angular velocity of the ball. It is calculated by $\omega = \frac{v}{r}$, and $v = \sqrt{\frac{6gl\sin\alpha_0}{5}}$ (see in Equation 2). The length l_1 on the slope represents the change in angular velocity (see in Equation 3).

2. **Dependent Variable**: The dependent variable in this investigation is the trajectory of the ball, measured in terms of horizontal displacement and vertical displacement.

3. **Control Variables**: The initial translational velocity is kept constant by adjusting l_2 (see in Equation 4); the nature of the ball (mass, surface, and radius) is kept constant by using the same ball; the initial projection angle and the releasing height are kept constant by using a fixed slope and platform; and the environmental conditions are kept constant by doing experiment in the same room.

5 Materials

1. **One ping pong ball**: the radius is approximately $0.020m \pm 0.0005m$.

2. **One slope**: partially covered by abrasive papers over a length l_1 that makes it rotate and partially covered by oil over a length l_2.

3. **Two threads**: with negligible thickness and friction but restricting the ball slide along a straight line.

6 Procedure for Data Collection

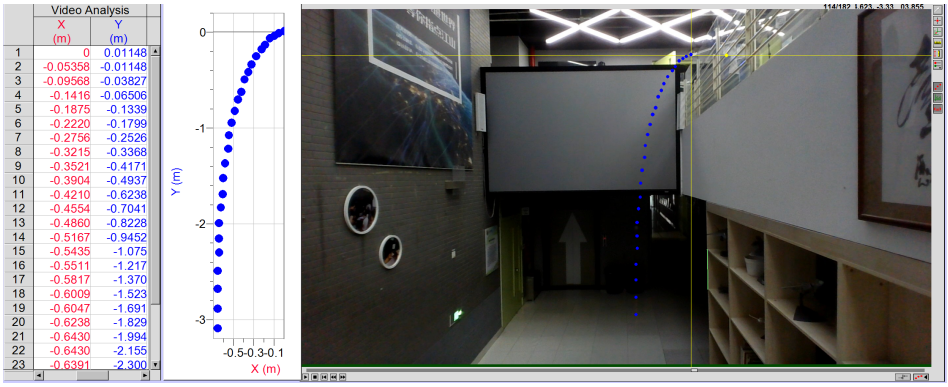

Figure 5: The Capture of Experiment and Video Analysis

The following steps will be undertaken to collect data:

1. **Set Up the Experiment**:
   Do this experiment in an indoor environment. Place the reference ruler ($0.479m \pm 0.0005m$) in the same plane with the slope, avoiding perspective distortion and ensuring proper scaling. Secure the slope on a high platform (in this experiment, the second floor). After properly aligning it, measure the slope's height and length to calculate the incline angle α_0.

2. **Prepare the High-Speed Camera**:
   Position the camera perpendicular to the slope to capture the entire descent of the ping pong ball. Ensure the camera remains fixed in position and height.

3. **Prepare Materials**:
   Prepare abrasive papers in particular length l_1 and paste them on the slope. Smear oil with length l_2 to help prevent rotation. Place two threads on the slope at an appropriate distance apart to guide the ball to move in a straight line. Use tape instead of glue to fix these materials, preventing the slope and ball surfaces from becoming wet. Mark the starting point on the slope where the ping pong ball will be released.

4. **Conduct the Experiment**:
   Place a ping pong ball at the starting point on the slope. Release the ball without imparting any extra spin. Record the ball's motion from release to the end of the motion. Repeat this step three times.

5. **Repeat for Different Spin Rates**:
   Perform five sets of trials in total, each with different angular velocities: adjusting the length of the abrasive paper l_1, while keeping the translational velocity consistent by adjusting the oil-covered length l_2 using Equation 4.

Note that start with the trial that has the greatest length of abrasive paper. This helps ensure the abrasive paper does not overlap with any previously oiled area, keeping the surface dry.

7 Ethical and Safety Concerns

1. Ensure that no one is in the vicinity where the ball will land. While I am responsible for releasing the ball from the high platform, my assistant will monitor the area to ensure safety.

2. Place a soft cushion or conduct the experiment on a grassy area where the ball lands to prevent damage. Damage to the ball, particularly through inelastic deformation, may affect its interaction with the air in subsequent trials.

8 Results/Raw Data

8.1 Independent Variable

l_1 / **m** $\pm$ 0.0005 **m**	l_2 / **m** $\pm$ 0.0005 **m**	ω / $rad \cdot s^{-1} \pm$ 0.0005 $rad \cdot s^{-1}$
1.000	0.051	95.207
0.800	0.094	85.156
0.600	0.160	73.747
0.400	0.260	60.214
0.200	0.427	42.578

Table 3: Releasing Position and Angular Velocity

8.2 Control Variable

Control Variable	**Value**	**Description**
α_0	$\arcsin(0.308)$	Angle of incline
ρ	$1.2\,\mathrm{kg\,m^{-3}}$	Air density
v_0	$2.458\,\mathrm{m\,s^{-1}}$	Initial translational velocity

Table 4: Control Variables

8.3 Dependent Variable (Raw Data)

A sample of collection of the displacement in x direction and y direction is shown ($95.207\,\mathrm{s^{-1}}$).

x / m $\pm$ 0.0005 m			y / m $\pm$ 0.0005 m		
trial 1	**trial 2**	**trial 3**	**trial 1**	**trial 2**	**trial 3**
-0.054	-0.058	-0.073	-0.011	-0.021	-0.036
-0.096	-0.095	-0.126	-0.038	-0.049	-0.069
-0.142	-0.140	-0.170	-0.065	-0.120	-0.118
-0.188	-0.186	-0.211	-0.134	-0.169	-0.170
-0.222	-0.231	-0.247	-0.180	-0.243	-0.223
-0.276	-0.260	-0.296	-0.253	-0.318	-0.296
-0.321	-0.301	-0.316	-0.337	-0.384	-0.369
-0.352	-0.334	-0.353	-0.417	-0.487	-0.478
-0.390	-0.359	-0.389	-0.494	-0.582	-0.564
-0.421	-0.388	-0.418	-0.624	-0.714	-0.677
-0.455	-0.417	-0.446	-0.704	-0.829	-0.779
-0.486	-0.450	-0.483	-0.823	-0.961	-0.892
-0.517	-0.478	-0.507	-0.945	-1.089	-1.058
-0.543	-0.495	-0.519	-1.075	-1.192	-1.196
-0.551	-0.516	-0.552	-1.217	-1.332	-1.322
-0.582	-0.528	-0.560	-1.370	-1.461	-1.480
-0.601	-0.548	-0.580	-1.523	-1.651	-1.642
-0.605	-0.565	-0.600	-1.691	-1.800	-1.829
-0.624	-0.573	-0.608	-1.829	-1.973	-1.975
-0.643	-0.590	-0.616	-1.994	-2.154	-2.169
-0.643	-0.590	-0.620	-2.155	-2.311	-2.332
-0.639	-0.594	-0.616	-2.300	-2.505	-2.502
-0.654	-0.590	-0.625	-2.491	-2.678	-2.709
-0.654	-0.594	-0.625	-2.679	-2.880	-2.911
-0.654	-0.594	-0.608	-2.885	-3.099	-3.118

Table 5: Trajectory Raw Data

9 Data Processing

9.1 Data Processing Procedure

1. **Uncertainty and Error bars**:
   - For each independent variable, three repeated trials are conducted. Although at a given time frame (defining time zero as the moment when the ball leaves the slope) the y values might not be exactly the same, they are generally close. The mean values x_{mean} and y_{mean} are calculated, and half-range values $\frac{x_{max}-x_{min}}{2}$ and $\frac{y_{max}-y_{min}}{2}$ are used as the error bars.
   - For example, in the first set of experiments, the three data points are $(-0.517, -0.945)$, $(-0.478, -1.089)$, and $(-0.507, -1.058)$. The average point is $(-0.501, -1.031)$. The x uncertainty is $\frac{-0.478+0.517}{2} \approx 0.02$, and the y uncertainty is $\frac{-0.945+1.089}{2} \approx 0.07$. Then, the average point with uncertainty is $(-0.50 \pm 0.02, -1.03 \pm 0.07)$.
   - Notice that for most of the data, the uncertainty among three repeated trials is greater than or equal to 0.01. The measurement error 0.0005 is negligible in comparison.
2. **Calculate Differences**:
   - For each y value in the experimental data, identify the data point with the closet y value from the simulation trajectory and calculate the percentage difference in x values:

$$\frac{|x_{exp} - x_{simul}|}{x_{simul}}. \tag{10}$$

3. **Plot Differences**:
   - Create a plot with experimental y values on the horizontal axis and the percentage difference in x values between the experimental and simulated trajectories on the vertical axis. It provides an intuitive view about how and where the experimental trajectory diverges from the ideal.

9.2 Processed Results

9.2.1 Difference Between Experimental With Simulation Results

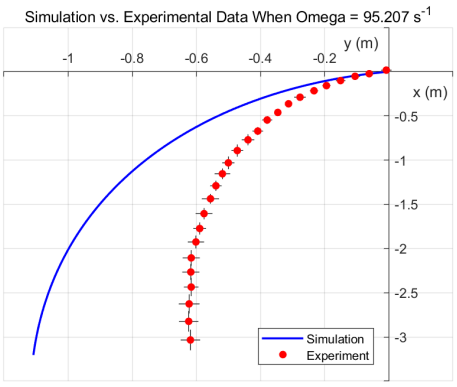

Figure 6: Experiment and Simulated Trajectory

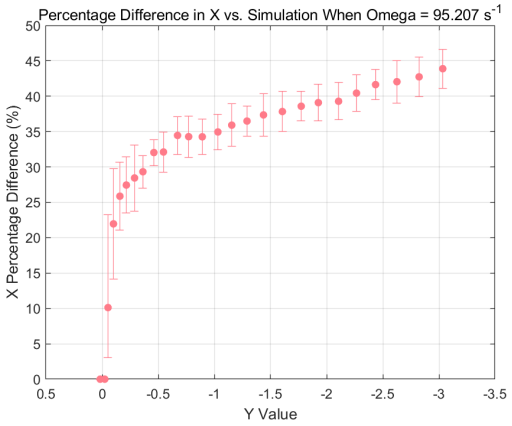

Figure 7: Percentage Differences Between Two Trajectory

A sample with an angular of velocity $95.207s^{-1}$ is shown above. Two sets of points (simulation and experimental results) are shown in Figure 6. The percentage difference between these two results is calculated using Equation 10 and shown in Figure 7. Note that the horizontal axis in Figure 7 is y values, since this figure shows how x percentage difference changes during the falling process—it is better to define y value as the independent variable in this figure.

9.3 Final Results

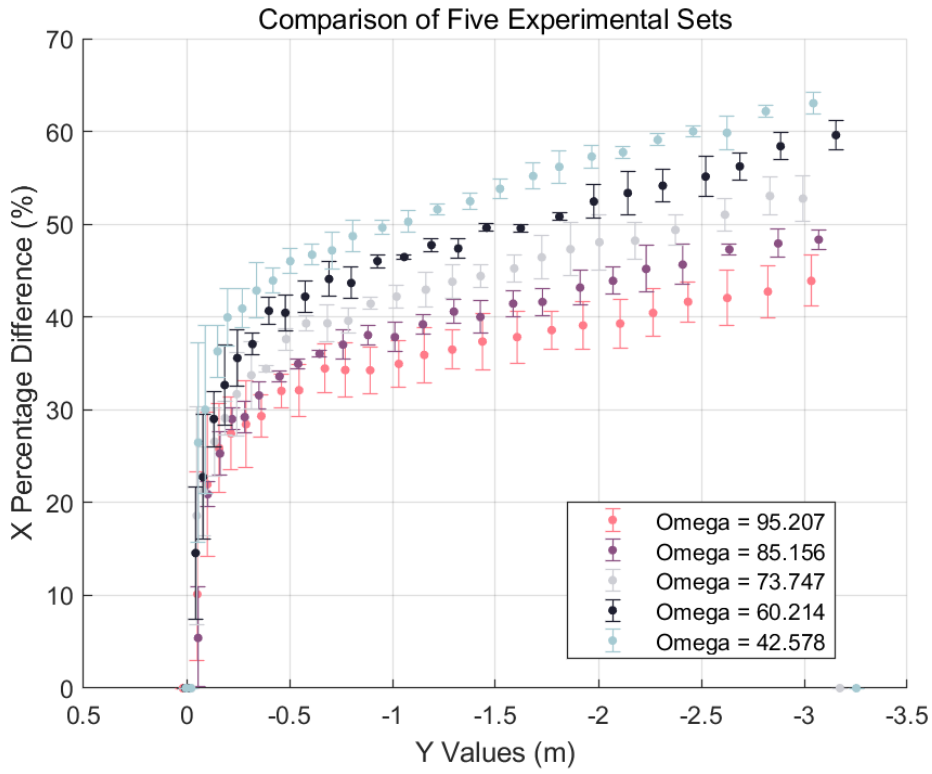

Figure 8: Comparison Among Five Experiments

Five sets of data are shown in Figure 8. For five sets of data, with the decrease of the displacement in y axis—moving faster and further from the origin—the theoretical-practical difference in the displacement in x axis approximately monotonically increases, meaning the divergence is larger during the motion. The extreme values near to the origin might be the unexpected random errors when point tracing using Logger Pro.

Also, within these sets of data, there is an monotonic relationship: with the increase of angular velocity, the trajectory is closer to the simulation results.

10 Conclusion

The angular velocity will influence the trajectory of the ball in the air, applying a Magnus force on the ball, making the ball shifting in the air. The result shows that this shift is not fully influenced by air drag force and buoyancy force, since the ball starts to "move back" when falling at a range between 3 m to 4 m in y axis—this phenomenon is special to Magnus effect.

In addition, this investigation into the effect of spin on the trajectory of a ping pong ball revealed that the decrease in spin rate almost leads to a consistent divergence from the simulated trajectory. The observed data showed a relatively monotonic relationship between the spin rate and the difference in trajectory: as the angular velocity increases, the trajectory is closer to the simulated results. This finding is contradictory with the hypothesis. An explanation to it is that with the decrease of angular velocity, the contact between the ball and the surrounding air is weaker and in reality than in simulation; this may lead to more unpredictable results and larger divergence than theory.

11 Discussion

The paper by Timkova [3] served as a significant inspiration for the series of experiments and simulations conducted in this study. Their work provided detailed, rigorous, and insightful theoretical foundations for understanding the Magnus effect. In contrast, this paper extends their research by conducting a more comprehensive set of experiments, varying the independent variable five times to explore the relationship between angular velocity and the trajectory. This study primarily offers an experimental basis for further investigation.

The practical relevance of this study could be improved by investigating scenarios involving higher ball speeds. According to *World Table Tennis*, professional players typically reach ball speeds of around $20\,\mathrm{km\,h^{-1}}$—approximately $72\,\mathrm{m\,s^{-1}}$—which is significantly higher than the speed considered in this investigation ($2.458\,\mathrm{m\,s^{-1}}$) [6].

11.1 Limitations and Suggested Improvements of this Investigation

11.1.1 Angular velocity

The angular velocity ω was assumed to be constant during the falling process. In reality, however, frictional forces from the surrounding air can affect ω. Timkova used a styrofoam ball (a solid sphere) with a radius of 0.05 m and a mass of 0.00936 kg, and found—via video analysis—that ω stayed nearly unchanged [3]. The moment of inertia of their styrofoam ball is $\frac{2}{5}mr^2 = 9.36 \times 10^{-5}\,\mathrm{kg\,m^2}$. In contrast, the ping pong ball (a hollow sphere) used in our experiment has a moment of inertia of $\frac{2}{3}mr^2 = 7.2 \times 10^{-6}\,\mathrm{kg\,m^2}$, which is only 7.8% of the value of the solid ball used by Timkova.

In Timkova's experiments, the experiment results matched the simulations well, with only minor percentage differences. By comparison, our results show a larger discrepancy. One major source of systematic error is the much lower moment of inertia of the ping pong ball. Because its inertia is smaller, its spin is more easily altered by air friction and thus does not remain constant.

This error can be mitigated by using a ball with a higher moment of inertia—such as a tennis ball, whose inertia typically ranges from about $1.6 \times 10^{-4}\,\mathrm{kg\,m^2}$ to $1.9 \times 10^{-4}\,\mathrm{kg\,m^2}$.

11.1.2 Rolling and sliding on the Slope

While abrasive paper can effectively prevent sliding, the oil-covered surface still provides enough friction to induce rolling. These two factors influenced the control of the initial translational velocity v_0. It has more influences on data sets with lower angular velocity, where the slope had a longer oil-covered section—thus reducing the initial translational velocity. One potential solution to it is to increase the length of the abrasive paper coverage while keeping the oil-covered portion the same. This reduces the influence by the oil-covered surface.

11.1.3 Measurement Inaccuracies

Manual collection of trajectory data introduced inaccuracies, since the 2D recording inevitably causes differences the 3D reality, regardless of the recording perspective. This experiment placed the camera at the mid point between the slope and the ground to minimize the standard deviation of the systematic errors, but the differences still existed. These systematic errors might be reduced by increasing the distance between the camera and the plane of ball movement.

Also, when using Logger Pro to manually mark points in videos, random errors occur because the marked positions may be slightly offset from the actual positions. The maximum x and y absolute uncertainty for this reason is 0.02 m, as the marked point always falls within the ball's radius of 0.02 m. Zooming out the video and using auxiliary lines to pinpoint the ball's geometric center can help decrease this uncertainty.

11.1.4 Air Property

Force coefficients, especially C_d and C_m, are determined by experiments [3] [7]. However, these experiments are complex and need precise measurement devices to ensure accuracy. This paper uses the values of the constants in Timkova's paper, which may potentially lead to a systematic uncertainty in essay.

Acknowledgments

I would like to thank my teacher, Dr. Yue Xu, for her guidance and feedback as my supervisor during the project, and my classmates, Wenxuan Ji and Yuanzhou Chen, for assisting in data collection during the experiment.

References

[1] Lyman J. Briggs. Effect of spin and speed on the lateral deflection of a baseball; and the magnus effect for smooth spheres. *American Journal of Physics*, 27:589, 1959.

[2] M.J. Carré S. Barber, S.B. Chin. Sports ball aerodynamics: A numerical study of the erratic motion of soccer balls. *Computers & Fluids*, 38:1091–1100, 2009.

[3] V. Timková and Z. Ješková. How magnus bends the flying ball - experimenting and modeling. *The Physics Teacher*, 55:112, 2017.

[4] Vassilios M. Spathopoulos. A spreadsheet model for soccer ball flight mechanics simulation. *Computers & Applied Engineering Education*, 19:508–513, 2011.

[5] Wolfram Frank Thorsten Kray, Jörg Franke. Magnus effect on a rotating soccer ball at high reynolds numbers. *Journal of Wind Engineering and Industrial Aerodynamics*, 124:46–53, 2014.

[6] World Table Tennis. How fast (or slow) are the pros. Accessed: 2025-04-08.

[7] Rod Cross. Aerodynamics of a party balloon. *The Physics Teacher*, 45(6):334–336, 2007.